Journal of Magnetism and Magnetic Materials 638 (2026) 173752

Contents lists available at ScienceDirect

Journal of Magnetism and Magnetic Materials

journal homepage: www.elsevier.com/locate/jmmm

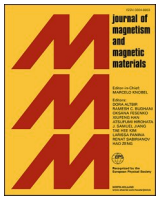

Effect of cyclic loading on the magnetic properties of FeCo-2V alloy

Sirapob Toyting [a,*], Christopher W. Harrison [b], Stefan Michalik [c], Alexis Lambourne [d], Howard J. Stone [a]

[a] University of Cambridge, Department of Materials Science and Metallurgy, 27 Charles Babbage Road, Cambridge CB3 0FS, UK
[b] Cardiff University, School of Engineering, Cardiff CF24 3AA, UK
[c] Diamond Light Source Ltd., Harwell Science and Innovation Campus, Didcot OX11 0DE, UK
[d] Rolls-Royce Plc, PO Box 2000, Derbyshire, DE24 7XX, UK

ARTICLE INFO

Keywords:
FeCo-2V alloy
Soft magnet
Cyclic loading
Coercivity
Core losses
Fatigue

ABSTRACT

FeCo-2V soft magnetic alloys offer attractive properties for demanding electromagnetic applications. While their magnetic properties are well-characterised under static loading conditions, the evolution of these properties under cyclic mechanical loading, as seen in service, remains insufficiently explored. This study examines how fatigue deformation alters the magnetic behaviour of an FeCo-2V alloy. The investigation employed strain-controlled cyclic loading combined with Single Sheet Tester measurements across multiple frequencies. A modified Bertotti loss separation analysis quantified the contributions of hysteresis and eddy current losses to total core loss. Experimental results demonstrated an increase in coercivity, and significant core loss increase during early-stage fatigue, followed by more gradual changes at higher cycle counts. The abrupt initial property changes correlate with rapid dislocation accumulation, while subsequent stabilisation reflects saturated defect densities. Notably, hysteresis losses dominated the degradation, while eddy current losses remained stable throughout cycling. These findings establish clear relationships between cyclic loading and magnetic properties in FeCo-2V and may serve as the basis for non-destructive fatigue assessment through magnetic measurements.

1. Introduction

The global transition to low-carbon electric transport has intensified demand for high-performance magnetic materials. In such applications, soft magnetic materials, including Fe—Si and Fe—Co alloys, are selected based on their saturation magnetisation, coercivity, and core loss characteristics. Among these, Fe—Co alloys with 2% vanadium (FeCo-2V) are particularly valuable due to their high saturation magnetisation (~2.35 T) and high Curie temperature (~950 °C) [1,2]. Despite their attractive properties, the high cost of FeCo-2V restricts its use to applications where higher performance justifies the expense, such as aerospace and high-efficiency electric vehicles [3].

Soft magnetic components in electric motors and generators routinely experience cyclic mechanical stress during operation. For example, low cycle fatigue from thermal cycling (one per machine switch-on) and high cycle fatigue from machine rotational loading and magnetostrictive effects (which may be several thousand rpm) [4,5]. These repeated loading conditions can induce fatigue damage that degrades both structural integrity and magnetic performance, potentially leading to unexpected device failure. Fatigue is a critical degradation mechanism in components subjected to cyclic loading and may lead to failure at stress levels significantly below the yield point [6]. This phenomenon makes fatigue particularly dangerous, as components may fail unexpectedly during normal service conditions.

Previous studies have shown that the fatigue life of FeCo-2V alloys is strongly influenced by microstructure, loading conditions, and deformation history. Studies by Mills et al. [7] and Keller et al. [8] using strain-controlled fatigue testing showed that FeCo-2V undergoes strain hardening, with cracks typically initiating at surface defects and propagating through transgranular cleavage. It was shown that the Coffin-Manson relationship, linking plastic strain amplitude to the number of cycles to failure, effectively described its low-cycle fatigue (LCF) behaviour. However, variations in heat treatment and grain structure can significantly alter its fatigue resistance.

The magnetic properties of ferromagnetic materials, particularly structural steels, have been widely studied under cyclic loading conditions due to their potential for non-invasive assessment of fatigue damage. As structural components in critical applications often

* Corresponding author.
E-mail address: st788@cam.ac.uk (S. Toyting).

https://doi.org/10.1016/j.jmmm.2025.173752
Received 24 July 2025; Received in revised form 22 November 2025; Accepted 8 December 2025
Available online 10 December 2025

experience repeated mechanical stresses during service, early detection of fatigue damage through changes in magnetic properties offers a promising alternative to conventional inspection methods. This is because magnetic parameters such as permeability and coercivity are sensitive to microstructural changes and residual stresses induced by cyclic deformation. For example, Deldar et al. [9] analysed changes in magnetic permeability in AISI 1045 steel and observed a reduction in maximum permeability with increasing stress cycles, a trend that was more pronounced at higher stress amplitudes. Similarly, Gorkunov et al. [10] investigated pipe steel under zero-to-tension cyclic loading and reported an increase in coercivity and a decrease in maximum permeability during the early stages of loading. These changes were attributed to residual stress accumulation along the tensile axis, which impeded magnetic domain wall motion. Zhang et al. [11] also identified comparable behaviour in ribbed steel under cyclic loading.

Building on this understanding, various non-destructive characterisation methods have been explored to assess fatigue damage in cyclically loaded components [12,13]. Magnetic techniques, in particular, have received growing attention due to the well-established link between magnetic and mechanical behaviour in ferromagnetic materials [14,15]. For instance, Barkhausen noise analysis has been employed to evaluate mechanical deformation in high-purity iron by Augustyniak et al. [16], and to assess fatigue damage in steels by Sagar et al. [17]. Despite these advancements, limited studies have explored the use of coercivity and power loss as fatigue indicators, especially in FeCo-2V alloys. Furthermore, the specific effects of cyclic loading on the magnetic properties of FeCo-2V remain largely underexplored.

To address this gap, the effects of cyclic loading on the magnetic properties of FeCo-2V alloys, focusing on core loss and coercivity, are investigated in this study. A combination of mechanical testing, magnetic Single Sheet Tester (SST) analysis, and loss separation methods is employed to characterise the changes in magnetic behaviour following cyclic deformation. This knowledge serves as a foundation for optimising these materials in magnetic applications where cyclic loading is a critical factor, and for developing magnetic-based indicators to monitor fatigue damage in service conditions.

2. Experimental procedures

2.1. Sample preparation and heat treatment

Vacodur 49 (nominal composition: 49 wt% Fe, 49 wt% Co, 2 wt% V) was supplied by Vacuumschmelze as cold-rolled sheets with dimensions of 0.2 mm (thickness) × 30 mm (width) × 300 mm (length). Before processing, the samples were cleaned in acetone to eliminate surface contaminants.

The samples were heated under flowing H_2 to 750 °C at a rate of 15 °C/min, followed by a 3-h isothermal hold to facilitate uniform recrystallisation and relieve internal stresses [18,19]. Cooling was performed at a controlled rate of 100–300 °C/h until ambient temperature was reached. This procedure followed standard commercial practices for mechanically optimised FeCo-2V [20].

This annealing route produces the mechanically optimised condition of FeCo-2V, which is widely used in commercial components that require a balance between high magnetic performance and adequate mechanical strength. While a magnetically optimised condition is sometimes preferred for applications demanding exceptionally low coercivity, it provides reduced strength and is less suitable for load-bearing rotating machinery. For context, a representative stress–strain curve for the mechanically optimised condition is provided in Fig. 1.

2.2. Cyclic loading pre-deformation

Cyclic deformation of the FeCo-2V samples was performed using an Instron 100 kN uniaxial servo-hydraulic mechanical testing system [21] equipped with hydraulic grips and an 8800MT controller on beamline I12-JEEP at Diamond Light Source. The tests were conducted under strain-controlled conditions, following parameters derived from previous fatigue studies on FeCo-2V alloys by Mills et al. [7] and Keller et al. [8]. A fully reversed sinusoidal waveform with a strain amplitude of 0.15%, frequency of 10 Hz, and stress ratio (R) of 0.1 was applied. Ten individual samples were tested, each subjected to a different predetermined cycle count: 0, 100, 500, 1000, 5000, 10,000, 25,000, 35,000, 50,000, and 75,000 cycles. Critically, a new sample was used for each cycle count, ensuring no cross-influence between datasets. These cycle counts represent 0% to 75% of the material's expected fatigue life under the applied test conditions [8]. These cycle counts were chosen to represent a range of fatigue states, with an emphasis on early-stage deformation, where previous research has indicated notable changes in magnetic properties [8]. This selection enabled the systematic investigation of how cyclic loading influences magnetic behaviour.

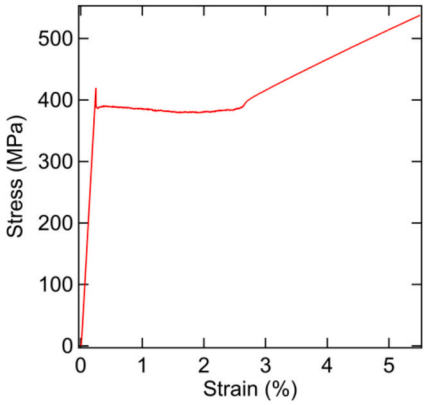

Fig. 1. Stress-strain curves of mechanically optimised FeCo-2V alloy.

2.3. Magnetic properties testing

The magnetic properties of the FeCo-2V alloy were measured using a Single Sheet Tester (SST). First, the AC magnetisation was applied to the samples using a waveform generated by a National Instruments DAQ PCI-6120, which was controlled by a LabVIEW interface to conform with IEC 60404–3 standards [22]. This waveform was then amplified *via* a Europower EP4000 amplifier and passed through an isolation transformer to eliminate any DC offset. The coil current (for H-field estimation) was derived from the voltage across a 0.49 Ω shunt resistor [23]. Simultaneously, the B-field (magnetic flux density) was measured using a sensing coil wound directly around the sample. The acquired data were processed in the control software to extract magnetic loss and permeability values from the resulting hysteresis loops [24,25].

For cyclic deformation studies, ten FeCo-2V strips were subjected to controlled fatigue loading before being mounted in the SST setup between yoke pairs. The frequency-dependent response was characterised by testing at eight frequencies ranging from 50 Hz to 800 Hz (50 Hz, 60 Hz, 70 Hz, 100 Hz, 200 Hz, 400 Hz, 600 Hz, and 800 Hz), enabling analysis of loss mechanisms. It should be noted that all magnetic measurements were performed *ex situ*, after the completion of cyclic loading. The fatigue tests were run continuously to the target cycle count without interruption, after which the pre-deformed samples were removed from the rig and directly tested in the SST.

2.4. Loss – Separation analysis

The total magnetic loss in FeCo-2V alloy was separated into three primary components: hysteresis loss (P_h), eddy current loss (P_{ed}), and excess loss (P_{ex}) assuming the linear combination of the components:

$$P_{total} = P_h + P_{ed} + P_{ex} \quad (1)$$

The Bertotti model [26] was employed to express these losses as functions of flux density (B) and frequency (f):

$$P_{\text{total}} = k_{\text{h}} B^{n} f + k_{\text{ex}} B^{3/2} f^{3/2} + k_{\text{ed}} B^{2} f^{2} \tag{2}$$

In which, k_{h}, k_{ed} and k_{ex} represent the material-specific coefficients for hysteresis, excess, and eddy current losses respectively, while n, the Steinmetz exponent, generally ranges from 1.5 to 2 for soft magnetic materials [26].

To simplify the parameter fitting, Eq. 2 was modified:

$$\frac{P_{\text{total}}}{f} = k_{\text{h}} B^{n} + k_{\text{ex}} B^{3/2} f^{1/2} + k_{\text{ed}} B^{2} f \tag{3}$$

This change enabled improved separation and extraction of each loss component during the fitting procedure [27,28].

2.5. EBSD – Kernel average Misorientation (KAM)

To characterise microstructural changes due to fatigue, EBSD was performed on the samples exposed to cyclic loading for 0, 35,000, and 75,000 cycles. Sample preparation consisted of successive grinding with *SiC* paper (grits: 600, 1200, and 2500), followed by multistep polishing using diamond suspensions of decreasing size (6 μm, 3 μm, 1 μm) followed by final polishing with colloidal silica (0.25 μm). During diamond polishing, an oil-based lubricant was applied to minimise oxidation, and samples were subsequently stored in a desiccator.

EBSD measurements were carried out using a Zeiss Gemini SEM 300 and an Oxford Instruments Symmetry detector, operating under 20 kV acceleration voltage, with a 60 μm aperture, 0.5 μm step size, and 4 ms per pixel dwell time. The working distance was 17.5 mm, and scans were performed on a 500 μm × 500 μm region, with the stage tilted at 70°. The collected data were analysed using MATLAB's MTEX toolbox to compute KAM values, providing a measure of fatigue-induced deformation across the three loading conditions.

3. Results

3.1. Magnetic properties testing

The magnetic response of FeCo-2V following cyclic loading demonstrated clear changes in hysteresis behaviour. Hysteresis loops from the samples that were subjected to 0, 5000, and 50,000 cycles are presented in Fig. 2 to illustrate representative changes. After 0 cycles, corresponding to the initial condition, the hysteresis loop exhibited a narrow profile with minimal area, indicating low energy loss during magnetisation. As the number of cycles increased, two notable changes were observed: a clockwise rotation of the loops and an expansion in their width. These modifications reflected increased resistance to magnetisation, as indicated by larger loop areas and greater coercivity.

The variation of coercivity as a function of loading cycles was quantified across all tested frequencies and is shown in Fig. 3. Coercivity increased progressively with the number of cycles, particularly in the early stages of cyclic loading. Across all frequencies, a sharp initial rise in coercivity was followed by a gradual increase, reaching a peak at 75,000 cycles. This trend was consistent with the observations from the hysteresis loop evolution.

Core loss results, displayed in Fig. 4, revealed a similar cycle-dependent behaviour. An increase in core loss was observed with rising cycle count, indicating higher energy dissipation in samples subjected to greater deformation. This pattern remained consistent across the full range of test frequencies, further emphasising the influence of cyclic loading on the magnetic performance of FeCo-2V alloys. For example, at 400 Hz (the frequency commonly used on aircraft fixed frequency generators) the loss increased by 31.4% at 50% of fatigue life compared with its start of life properties.

To further analyse the trend, linear regressions were applied to both

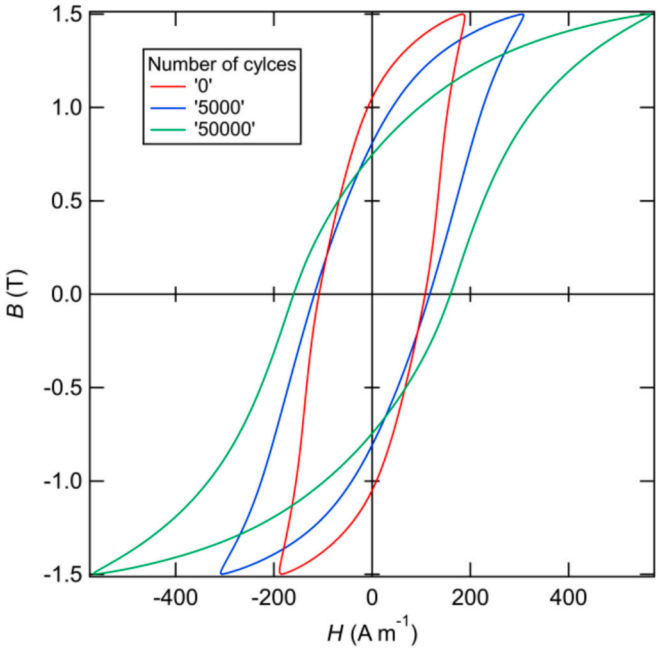

Fig. 2. Hysteresis loops of the FeCo-2V samples subjected to 0, 5000 and 50,000 loading cycles (test frequency = 50 Hz). H denotes the applied magnetic field strength (A·m^{-1}), and B denotes the magnetic flux density (T).

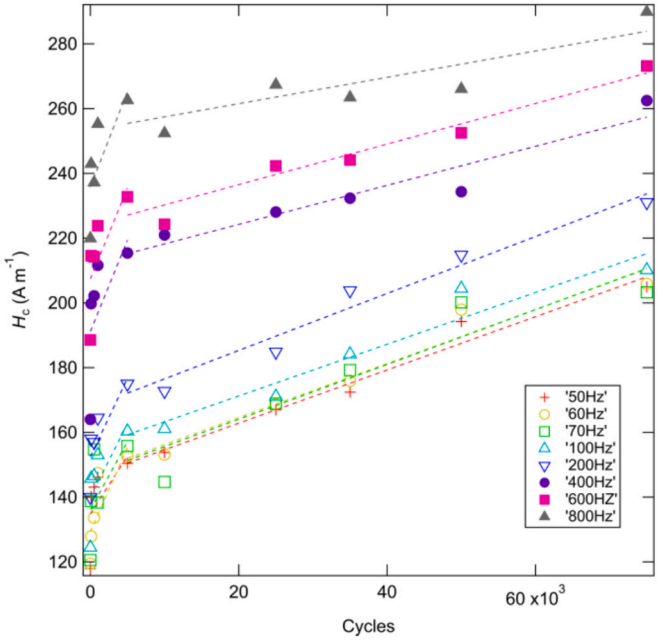

Fig. 3. Coercivity of FeCo-2V against number of loading cycles at different frequencies.

the coercivity and core loss data, segmented into two intervals: 0–5000 cycles and 5000–75,000 cycles. As shown in Figs. 3 and 4, the trendlines fitted to the 0–5000 cycle range exhibited steeper slopes than those fitted to the 5000–75,000 cycle range at all frequencies.

3.2. Loss-separation analysis

To investigate the contributions of different energy loss mechanisms in relation to cyclic loading, a loss-separation analysis was performed. The modified Bertotti equation (Eq. 3) was used to plot total loss per

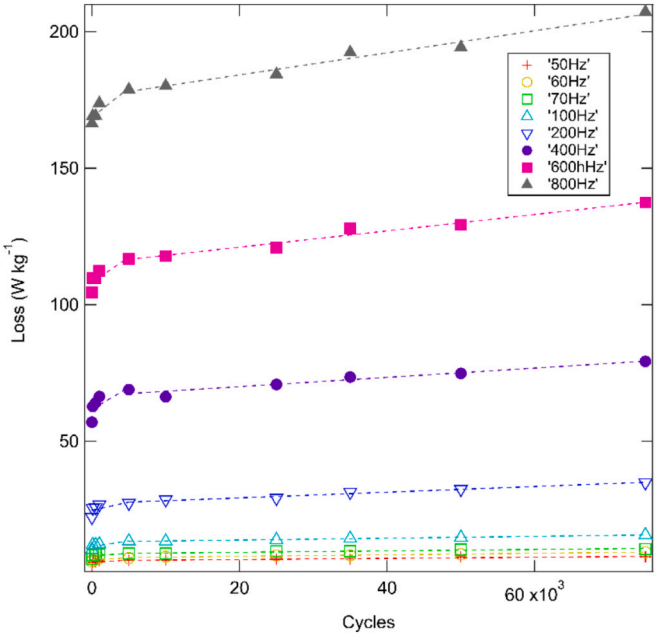

Fig. 4. Core loss of FeCo-2V against number of loading cycles at different frequencies.

frequency ($\frac{P_{total}}{f}$) against the square root of frequency ($f^{1/2}$), producing a quadratic relationship expressed as $y = k_0 + k_1 x + k_2 x^2$. A quadratic fit was applied to each dataset at a constant magnetic flux density of 2 T. An example of this fitting process is presented in Fig. 5, with the fitting coefficients k_0, k_1 and k_2 subsequently extracted for further analysis.

The hysteresis loss coefficient (k_h), excess loss coefficient (k_{ex}) and the eddy current loss coefficient (k_{ed}) were derived from the fitting parameters k_0, $k_1$and k_2 respectively. These coefficients were then plotted against the number of loading cycles, as illustrated in Fig. 6. An increasing trend in the hysteresis loss coefficient was observed over the course of cyclic loading, with values rising from 0.10 to 0.15 between 0 and 75,000 cycles, respectively (Fig. 6a). Furthermore, the hysteresis

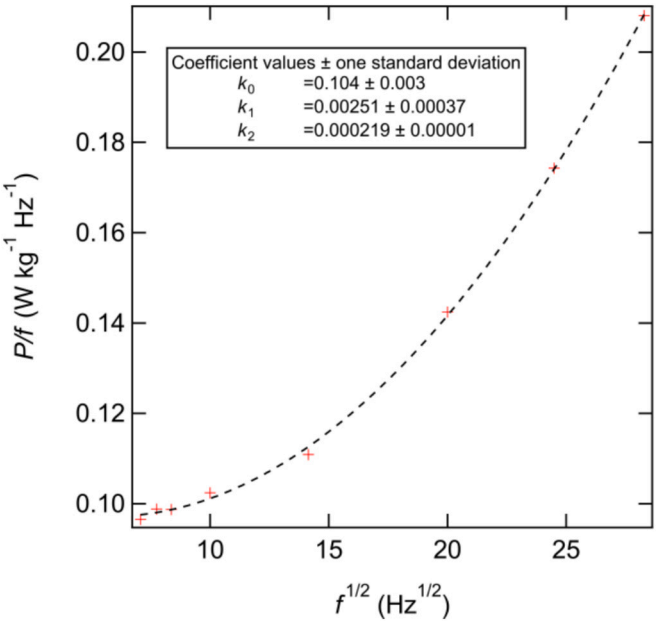

Fig. 5. Example of loss separation analysis plot of the FeCo-2V sample at 0 cycle ($B = 2$ T).

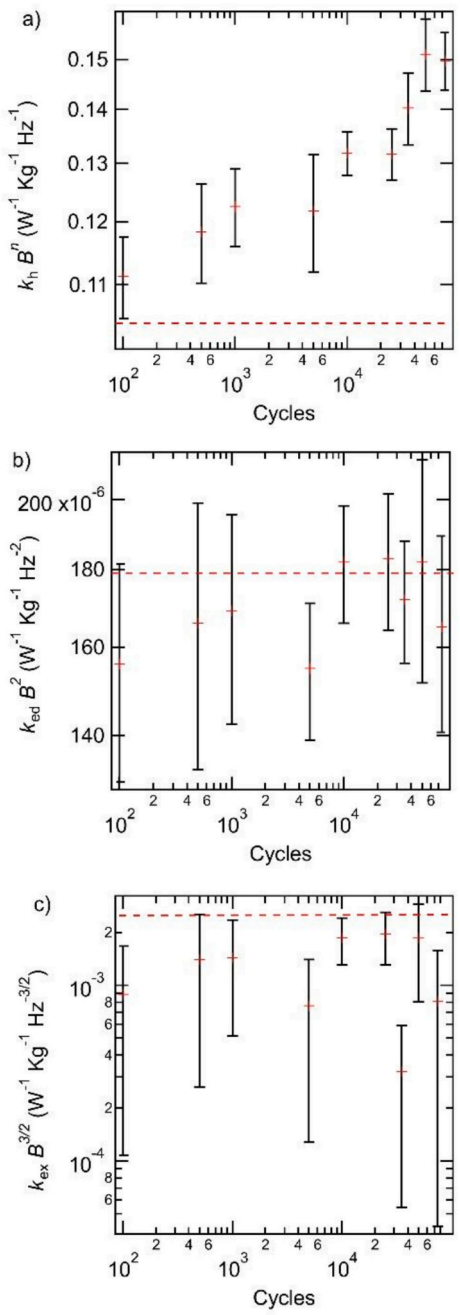

Fig. 6. Plots of loss coefficients of FeCo-2V against number of loading cycles. Red dash line represents value at 0 cycle. (a) hysteresis loss coefficient (b) eddy current loss coefficient and (c) excess loss coefficient. (For interpretation of the references to colour in this figure legend, the reader is referred to the web version of this article.)

loss coefficient was significantly larger than both the eddy current and excess loss coefficients.

The eddy current loss coefficient (Fig. 6b) displayed only minor fluctuations across the full range of loading cycles, with values remaining between 1.50×10^{-4} and 1.85×10^{-4} and no discernible upward or downward trend. Similarly, the excess loss coefficient (Fig. 6c) showed no systematic variation, fluctuating slightly between 0.8×10^{-3} and 2.5×10^{-3} over the same cycles.

3.3. EBSD – Kernel average Misorientation (KAM)

Electron Backscatter Diffraction (EBSD) was employed to assess the

microstructural change of FeCo-2V samples subjected to 0, 35,000, and 75,000 cycles of cyclic loading. The EBSD data were processed using the MTEX toolbox to generate Kernel Average Misorientation (KAM) maps, with the resulting misorientation angle distributions illustrated as violin plots in Fig. 7. In these plots, red diamond markers denote the mean values, while black contours depict the spread of misorientation angles within each sample.

The results revealed that increased cyclic loading led to broader distributions of misorientation angles, indicating greater microstructural heterogeneity. Higher cycle counts corresponded to both elevated average misorientation angles and a higher number of high angle misorientations. Specifically, the mean misorientation angles increased from 0.38° at 0 cycles to 0.74° at 35,000 cycles and 0.81° at 75,000 cycles.

4. Discussion

The findings of this study provide insights into the effect of cyclic loading on the magnetic properties of FeCo-2V alloys. While all tested samples exhibited similarly shaped hysteresis loops, noticeable differences were observed with increasing loading cycles. Specifically, the hysteresis loop of the sample subjected to 50,000 loading cycles displayed a significantly larger area compared to those cycled at 0 and 5000 cycles, indicating higher magnetic energy dissipation. This observation was consistent with core loss measurements, where the highest core losses was recorded after 75,000 loading cycles.

The increase in total core loss with additional loading cycles can be attributed primarily to a rise in hysteresis loss, as supported by the coercivity data. Coercivity exhibited a gradual and consistent rise with increasing loading cycles, indicating a greater resistance to magnetisation. This trend is attributed to fatigue-induced hardening, as coercivity is known to indirectly correlate with microstructural strengthening mechanisms, particularly dislocation accumulation, which impedes domain wall motion and increases the energy required for magnetisation [29].

These observations are consistent with the results of the loss-separation analysis. The hysteresis loss coefficient (k_h) increased steadily with the number of loading cycles, while the eddy current loss coefficient (k_{ed}) and excess current loss coefficient (k_{ex}) remained relatively unchanged. Although k_h shows a clear rise and exceeds the magnitudes of both k_{ed} and k_{ex}, in this study, it is important to note that classical eddy current loss typically scale with the square of frequency and are often the dominant contribution at higher frequencies [30,31]. However, in this case, k_{ed} remained nearly constant, consistent with the fact that eddy current loss is primarily governed by sample geometry, thickness, and electrical resistivity, all of which were minimally affected by the fatigue loading. The relatively stable k_{ed} values therefore confirm that the observed increase in total core loss was predominantly driven by a rise in k_h.

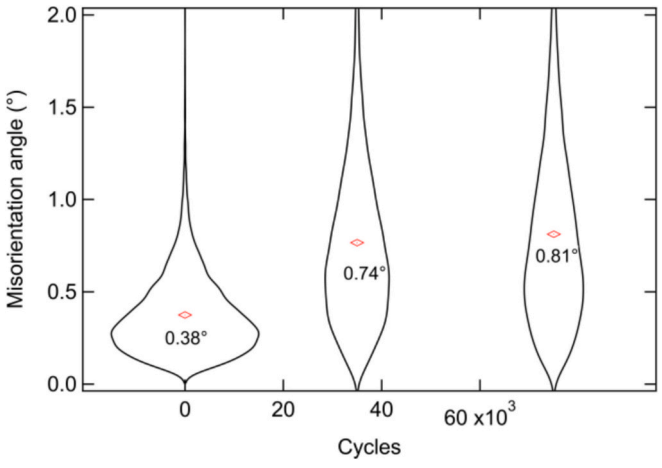

Fig. 7. A violin distribution plot of average misorientation angle against number of loading cycles.

Hysteresis loss coefficient (k_h) is influenced by domain wall mobility [31], its increase implies restricted domain wall movement, likely due to the accumulation of dislocations. This interpretation is supported by the EBSD-KAM results, which show an increase in the average misorientation angle with more loading cycles, consistent with a rise in dislocation density. These dislocations act as pinning sites, impeding domain wall motion and leading to increased hysteresis loss, higher coercivity, and greater total core loss, consistent with previous studies [24,32–36].

A limitation of the present methodology is that SST measurements were performed on the full strip length, including the grip regions. Grip indentation may therefore introduce a minor secondary contribution to the measured magnetic response. However, EBSD–KAM analysis conducted within the gauge section shows clear and progressive increases in misorientation with cycle count, consistent with dislocation accumulation. These trends align directly with the observed increases in coercivity and hysteresis loss, indicating that fatigue-induced microstructural evolution in the gauge region is the dominant contributor to magnetic degradation, rather than grip effects.

Prior to loading, the dislocation density in the material was low, as expected following the annealing heat treatment. However, during the early stages of fatigue, rapid plastic strain accumulation led to a substantial increase in dislocation density. This is evidenced by the EBSD-KAM results, which show a notable rise in the misorientation angle between the sample at 0 cycles and the one at 35,000 cycles. Similar observations have been reported by Gorkunov et al. [10] and Devine et al. [37], who found a sharp increase in coercivity during the early stages of fatigue in ferromagnetic steels. The increase in dislocation density was identified as the primary factor contributing to the initial rise in coercivity.

This rapid magnetic degradation in the early fatigue stage is further supported by linear regression analysis of coercivity and core loss data, which was segmented into two regions: 0–5000 cycles and 5000–75,000 cycles. The trendlines fitted to the early stage (0–5000 cycles) consistently exhibited steeper gradients than those in the later stage (5000–75,000 cycles) across all test frequencies. The steeper initial slope reflects a faster rate of increase in magnetic losses and coercivity.

Supplementary monotonic loading tests were performed to assess whether single-step plastic deformation could produce magnetic changes comparable to cyclic loading. Monotonic straining to 0.3% resulted in only modest increases in coercivity (~120 $A{\cdot}m^{-1}$) and core loss (~10 $W{\cdot}kg^{-1}$), whereas cyclic loading produced substantially larger changes under the same peak strain amplitude. This confirms that progressive fatigue damage, rather than monotonic plastic deformation, is the primary mechanism responsible for the magnetic degradation observed in this study.

Further support for this behaviour can be found in the study by Makowska et al. [38]. In their study, an increase in Barkhausen noise was reported during early fatigue in ferromagnetic steels, reflecting heightened domain wall pinning. Since Barkhausen noise originates from discontinuous domain wall motion and is highly sensitive to changes in microstructure and local stress state of the material [39], its rise is also indicative of increased dislocation activity and microcrack development [40].

In the mid-stage of fatigue life, only marginal increases in plastic strain were observed. By this stage, the dislocation density had almost reached a stable, saturated level, resulting in minimal further accumulation. This is reflected in the EBSD-KAM results, which showed only a slight increase in the misorientation angle between the samples at 35,000 and 75,000 cycles. As a result, both coercivity and core loss exhibited no significant increases during this phase. This trend is further supported by the reduced gradient in the linear regression fits beyond 5000 cycles, indicating a slower rate of magnetic property degradation.

These findings are consistent with previous observations in ferromagnetic steels [10,37].

Zhang et al. [11] similarly reported pronounced changes in magnetisation during the early stage of fatigue, followed by stability in the mid-life period. Their study also indicated a significant change in magnetisation in the final fatigue stage due to magnetic flux leakage at fatigue cracks. In this phase, crack expansion leads to accumulation of magnetic fields and the formation of leakage magnetic fields, which disturb the local magnetic field at the cracks and produce abrupt variations in magnetisation. However, this phenomenon was not observed in the current study, as the samples were only tested up to 75% of their estimated fatigue life and no visible macroscopic cracks were detected.

It is important to consider the extent to which the present findings on thin foils can be extrapolated to bulk FeCo-2V components. The 0.2 mm foil geometry used in this study is directly relevant to laminated electrical-steel architectures, where thin sheets are required to minimise eddy currents. In such applications, the fatigue–magnetic coupling observed here is expected to be directly applicable.

In contrast, bulk geometries such as round bars ($\geq$ 6 mm diameter) develop fatigue damage that is often concentrated near the surface, while the interior experiences minimal deformation. Consequently, the undamaged interior dominates the overall magnetic response, reducing the sensitivity of bulk measurements to early-stage fatigue when compared with foils. Nevertheless, the underlying mechanism identified here, fatigue-induced dislocation accumulation restricting domain wall motion, remains intrinsic to FeCo-2V and should produce qualitatively similar trends in bulk, albeit with smaller magnitude.

5. Conclusion

This study systematically investigated the effects of cyclic loading on the magnetic properties of FeCo-2V alloys through strain-controlled fatigue testing and magnetic characterisation. The key findings demonstrate that cyclic loading significantly alters the magnetic behaviour of FeCo-2V, with distinct trends observed for different loss mechanisms.

The results reveal that cyclic loading induces substantial changes in hysteresis properties, evidenced by the expansion of hysteresis loops and a progressive increase in coercivity with accumulated cycles. The hysteresis loss coefficient exhibited a significant rise over 75,000 cycles, directly correlating with the observed magnetic hardening. In contrast, the eddy current loss coefficient remained relatively stable, indicating minimal impact of cyclic deformation on bulk electrical conductivity. These findings provide clear experimental evidence that magnetic degradation in fatigue FeCo-2V is primarily driven by microstructural changes affecting domain wall motion rather than macroscopic conductivity.

The significance of this work lies in its demonstration of the critical relationship between mechanical fatigue which may be seen in service and magnetic performance in FeCo-2V soft magnetic alloys. By quantifying how different magnetic properties change with cyclic loading, this research provides essential data for designing FeCo-2V components in applications subject to cyclic loading and for effort to use changes in magnetic properties to monitor fatigue damage in FeCo-2V alloy.

CRediT authorship contribution statement

Sirapob Toyting: Writing – original draft, Visualization, Project administration, Investigation, Formal analysis, Conceptualization. **Christopher W. Harrison:** Writing – review & editing, Supervision, Methodology, Investigation. **Stefan Michalik:** Writing – review & editing, Methodology, Investigation. **Alexis Lambourne:** Writing – review & editing, Resources, Funding acquisition. **Howard J. Stone:** Writing – review & editing, Supervision, Project administration, Funding acquisition, Conceptualization.

Declaration of generative AI and AI-assisted technologies in the writing process

During the preparation of this work the authors used ChatGPT in order to improve grammar. After using this tool/service, the authors reviewed and edited the content as needed and take full responsibility for the content of the publication.

S. Toyting reports financial support was provided by Royal Thai Government Ministry of Science and Technology. S. Toyting reports financial support was provided by Rolls-Royce plc. If there are other authors, they declare that they have no known competing financial interests or personal relationships that could have appeared to influence the work reported in this paper.

Declaration of competing interest

The authors declared that they have no known competing financial interests or personal relationships that could have appeared to influence the work reported in this paper.

Acknowledgments

This work was financially supported by Royal Thai government scholarship and Rolls-Royce plc. We acknowledge Diamond Light Source for offline time on beamline I12-JEEP.

Data availability

Data will be made available on request.

References

[1] R. Hilzinger, W. Rodewald, Magnetic domains and process of magnetization, in: Magnetic Materials: Fundamentals, Products, Properties, and Applications, VAC, VACUUMSCHMELZE Erlangen, Hanau, Germany, Erlangen, Hanau, Germany: Publicis, 2013, pp. 45–72.
[2] G. Herzer, Modern soft magnets: amorphous and nanocrystalline materials, Acta Mater. 61 (3) (2013) 718–734, https://doi.org/10.1016/j.actamat.2012.10.040.
[3] S. Tumanski, Handbook of Magnetic Measurements, 0 ed., CRC Press, 2016 https://doi.org/10.1201/b10979.
[4] J. Karthaus, S. Steentjes, D. Gröbel, K. Andreas, M. Merklein, K. Hameyer, Influence of the mechanical fatigue progress on the magnetic properties of electrical steel sheets, Arch. Electr. Eng. 66 (2) (2017) 351–360, https://doi.org/10.1515/aee-2017-0026.
[5] E. Sikanen, J. Nerg, J.E. Heikkinen, M. Gerami Tehrani, J. Sopanen, Fatigue life calculation procedure for the rotor of an embedded magnet traction motor taking into account thermomechanical loads, Mech. Syst. Signal Process. 111 (2018) 36–46, https://doi.org/10.1016/j.ymssp.2018.03.055.
[6] R. G. Budynas and J. K. Nisbett, 'Fatigue failure resulting from variable loading', in Shigley's Mechanical Engineering Design, 9th ed., McGraw-Hill, pp. 265–357.
[7] M.J. Mills, et al., Characterizing the fatigue behavior of wrought Fe–co–2V using experimental techniques, J. Eng. Mater. Technol. 144 (3) (2022) 031008, https://doi.org/10.1115/1.4054142.
[8] E. Keller, T.A. Khraishi, K.L. Johnson, Mechanical Characterization of Fe-Co-2V (Hiperco): Fatigue/Monotonic Testing, Hardness Testing and Fractography, 2020. Available: https://api.semanticscholar.org/CorpusID:224970350.
[9] S. Deldar, M. Smaga, T. Beck, On the influence of cyclic loadings on the magnetic permeability of ferritic-pearlitic AISI 1045 steel, Int. J. Fatigue 159 (2022) 106650, https://doi.org/10.1016/j.ijfatigue.2021.106650.
[10] E. Gorkunov, A. Povolotskaya, S. Zadvorkin, E. Putilova, A. Mushnikov, Effect of cyclic loading on the magnetic behavior of hot-rolled pipe steel 08G2B, Procedia Struct. Integr. 20 (2019) 4–8, https://doi.org/10.1016/j.prostr.2019.12.107.
[11] D. Zhang, W. Huang, J. Zhang, W. Jin, Y. Dong, Prediction of fatigue damage in ribbed steel bars under cyclic loading with a magneto-mechanical coupling model, J. Magn. Magn. Mater. 530 (2021) 167943, https://doi.org/10.1016/j.jmmm.2021.167943.
[12] D. Burzic, J. Zamberger, E. Kozeschnik, Non-destructive evaluation of decarburization of spring steel using electromagnetic measurement, NDT E Int. 43 (5) (2010) 446–450, https://doi.org/10.1016/j.ndteint.2010.04.006.
[13] I. Altpeter, R. Becker, G. Dobmann, R. Kern, W. Theiner, A. Yashan, Robust solutions of inverse problems in electromagnetic non-destructive evaluation, Inverse Probl. 18 (6) (2002) 1907, https://doi.org/10.1088/0266-5611/18/6/328.
[14] J. Tenkamp, M. Haack, F. Walther, M. Weibring, P. Tenberge, Application of micromagnetic testing systems for non-destructive analysis of wear progress in case-hardened 16MnCr5 gear wheels, Mater. Test. 58 (9) (2016) 709–716, https://doi.org/10.3139/120.110924.

[15] O. Perevertov, R. Schäfer, Influence of applied tensile stress on the hysteresis curve and magnetic domain structure of grain-oriented Fe–3%Si steel, J. Phys. D. Appl. Phys. 47 (18) (2014) 185001, https://doi.org/10.1088/0022-3727/47/18/185001.
[16] B. Augustyniak, L. Piotrowski, M. Chmielewski, K. Kosmas, E. Hristoforou, Barkhausen noise properties measured by different methods for deformed Armco samples, IEEE Trans. Magn. 46 (2) (2010) 544–547, https://doi.org/10.1109/TMAG.2009.2033340.
[17] S. Sagar, N. Parida, S. Das, G. Dobmann, D. Bhattacharya, Magnetic Barkhausen emission to evaluate fatigue damage in a low carbon structural steel, Int. J. Fatigue 27 (3) (2005) 317–322, https://doi.org/10.1016/j.ijfatigue.2004.06.015.
[18] T. Sourmail, Evolution of strength and coercivity during annealing of FeCo based alloys, Scr. Mater. 51 (6) (2004) 589–591, https://doi.org/10.1016/j.scriptamat.2004.05.028.
[19] Z. Li, Z. Chen, J.T. Oh, V. Gill, A. Lambourne, Improving the mechanical and magnetic properties of Equiatomic FeCo-2V alloy through mild magnetic field annealing, Metall. Mater. Trans. A 55 (10) (2024) 4061–4071, https://doi.org/10.1007/s11661-024-07527-0.
[20] R. Hilzinger, W. Rodewald, Crystalline soft magnetic materials and ductile permanent magnets, in: Magnetic Materials: Fundamentals, Products, Properties, and Applications, VAC, VACUUMSCHMELZE Erlangen, Hanau, Germany, Erlangen, Hanau, Germany: Publicis, 2013, pp. 207–246.
[21] S.J. Moorhouse, N. Vranješ, A. Jupe, M. Drakopoulos, D. O'Hare, The Oxford-diamond *in situ* cell for studying chemical reactions using time-resolved X-ray diffraction, Rev. Sci. Instrum. 83 (8) (2012) 084101, https://doi.org/10.1063/1.4746382.
[22] IEC 60404–3:2022, Magnetic materials - Part 3: Methods of measurement of the magnetic properties of electrical steel strip and sheet by means of a single sheet tester, Nov. 08, 2022.
[23] P. Anderson, Measurement techniques for the assessment of materials under complex magnetising conditions, Przeglad Elektrotechniczny 87 (2011) 61–64.
[24] A. Daem, P. Sergeant, L. Dupré, S. Chaudhuri, V. Bliznuk, L. Kestens, Magnetic properties of silicon steel after plastic deformation, Materials 13 (19) (2020) 4361, https://doi.org/10.3390/ma13194361.
[25] S.G. Ghalamestani, T. Hilgert, S. Billiet, L. Vandevelde, J.A. Melkebeek, J.J. J. Dirckx, Measurement of magnetostriction using dual laser heterodyne interferometers: experimental challenges and preliminary results, 2009. Available: https://api.semanticscholar.org/CorpusID:67840177.
[26] D. Jiles, Soft Magnetic Materials, in: Introduction to Magnetism and Magnetic Materials, 3rd ed., CRC Press, Boca Raton, 2015, pp. 321–326.
[27] K. Yamazaki, N. Fukushima, Iron-loss modeling for rotating machines: comparison between Bertotti's three-term expression and 3-D Eddy-current analysis, IEEE Trans. Magn. 46 (8) (2010) 3121–3124, https://doi.org/10.1109/TMAG.2010.2044384.
[28] T. Wang, J. Yuan, Improvement on loss separation method for Core loss calculation under high-frequency sinusoidal and nonsinusoidal excitation, IEEE Trans. Magn. 58 (8) (2022) 1–9, https://doi.org/10.1109/TMAG.2022.3187206.
[29] C.C.H. Lo, F. Tang, Y. Shi, D.C. Jiles, S.B. Biner, Monitoring fatigue damage in materials using magnetic measurement techniques, J. Appl. Phys. 85 (8) (1999) 4595–4597, https://doi.org/10.1063/1.370419.
[30] W. Pieper, J. Gerster, Total power loss density in a soft magnetic 49% co–49% Fe–2% V-alloy, J. Appl. Phys. 109 (7) (2011) 07A312, https://doi.org/10.1063/1.3537956.
[31] R. Hilzinger, W. Rodewald, The magnetic circuit - basic relationships between magnetic and electrical terms, in: Magnetic Materials: Fundamentals, Products, Properties, and Applications, VAC, VACUUMSCHMELZE Erlangen, Hanau, Germany, Erlangen, Hanau, Germany: Publicis, 2013, pp. 103–137.
[32] Ferromagnetism, in: Introduction to Magnetic Materials, John Wiley & Sons, Ltd, 2008, pp. 115–149, https://doi.org/10.1002/9780470386323.ch4.
[33] N.A. Spaldin, Ferromagnetic domains', in: Magnetic Materials: Fundamentals and Applications, Cambridge University Press, 2010, pp. 79–95.
[34] B.D. Cullity, C.D. Graham, Introduction to Magnetic Materials, 1st ed., Wiley, 2008 https://doi.org/10.1002/9780470386323.
[35] R. Hilzinger, W. Rodewald, Magnetization process, in: Magnetic Materials: Fundamentals, Products, Properties, and Applications, VAC, VACUUMSCHMELZE Erlangen, Hanau, Germany, Erlangen, Hanau, Germany: Publicis, 2013, pp. 58–72.
[36] O. Hubert, E. Hug, I. Guillot, M. Clavel, Effect of internal stresses and dislocation features on the magnetic properties of soft ferromagnetic materials, J. Phys. IV 08 (PR2) (1998) Pr2-515–Pr2-518, https://doi.org/10.1051/jp4:19982119.
[37] M.K. Devine, D.A. Kaminski, L.B. Sipahi, D.C. Jiles, Detection of fatigue in structural steels by magnetic property measurements, J. Mater. Eng. Perform. 1 (2) (1992) 249–253, https://doi.org/10.1007/BF02648624.
[38] K. Makowska, T. Szymczak, Z.L. Kowalewski, Fatigue behaviour of medium carbon steel assessed by the Barkhausen noise method, Acta Mech. Autom. 18 (1) (2024) 40–47, https://doi.org/10.2478/ama-2024-0005.
[39] K. Tiitto, Use of Barkhausen noise in fatigue, in: D.O. Thompson, D.E. Chimenti (Eds.), Review of Progress in Quantitative Nondestructive Evaluation, Springer US, Boston, MA, 1990, pp. 1845–1853, https://doi.org/10.1007/978-1-4684-5772-8_237.
[40] Y. Tomita, K. Hashimoto, and N. Osawa, 'Nondestructive estimation of fatigue damage for steel by Barkhausen noise analysis'.n.d.